PATCHY DISTRIBUTION OF ANCIENT, LUNAR ICE CONTRASTS WITH YOUNG, COHERENT ICE DEPOSITS ON MERCURY. Ariel N. Deutsch[1], James W. Head[1], and Gregory A. Neumann[2], [1]Department of Earth, Environmental and Planetary Sciences, Brown University, Providence, RI 02912 (ariel_deutsch@brown.edu), [2]NASA Goddard Space Flight Center, Greenbelt, MD 20771, USA.

Introduction: The poles of Mercury and the Moon both show evidence for water ice, but the deposits on Mercury have a greater areal distribution [1] and a more pure concentration [2]. Earth-based radar observations revealed an estimated ~25,000 m^2 of ice at Mercury's poles [1] that was modeled to be ~95 wt. % pure [2]. Images [3] and reflectance measurements [4] acquired by the MErcury Surface, Space ENvironment, GEochemistry, and Ranging (MESSENGER) spacecraft showed that these deposits are spatially homogeneous within permanently shadowed regions (PSRs).

In contrast to the relatively pure water-ice deposits on Mercury [2], volatile deposits on the Moon are rather heterogeneous. For instance, multiple volatiles species were detected in the ejecta plume of the LCROSS experiment that impacted into Cabeus at the Moon's south pole, suggesting that the deposits are not pure water ice [5–6]. Additionally, mapping of UV albedo spectra and surface temperature revealed a highly spatially heterogeneous distribution of water frost within PSRs [7].

Impact gardening and space weathering [8] can produce spatial heterogeneities because these processes cause loss and redistribution of volatiles through time. Impacts introduce heterogeneity into the system because they remove volatiles via vaporization, and also preserve volatiles through the emplacement of ejecta, with a net effect of breaking up and burying the ice through time [9]. Because these processes take time, the degree of heterogeneity is inherently related to the age of the ice.

Here, we explore how the differences in purity and spatial heterogeneity of surface ice at Mercury and the Moon may be related to the ages of the ice.

Methodology: *Age estimates of water-ice deposits on Mercury.* Using images acquired by the Wide-Angle Camera during MESSENGER's low-altitude campaign [10], we identify small craters in the PSRs that are correlated with high reflectance, suggestive of excavated material. While the majority of craters observed in the PSRs may be pre-existing topography emplaced before the deposition of the ice [e.g., 11], the anomalous small craters associated with high-reflectance material may have formed after the emplacement of the ice. If so, then these small craters superposing the ice deposit can be used to date the ice surface itself. Here, we estimate the absolute ages of specific mercurian ice deposits (Fig. 1) using small, superposed craters associated with high-reflectance rings. Absolute ages of Laxness, Bechet, and Ensor craters are estimated using CraterstatsII [12] and chronology and production systems from [13].

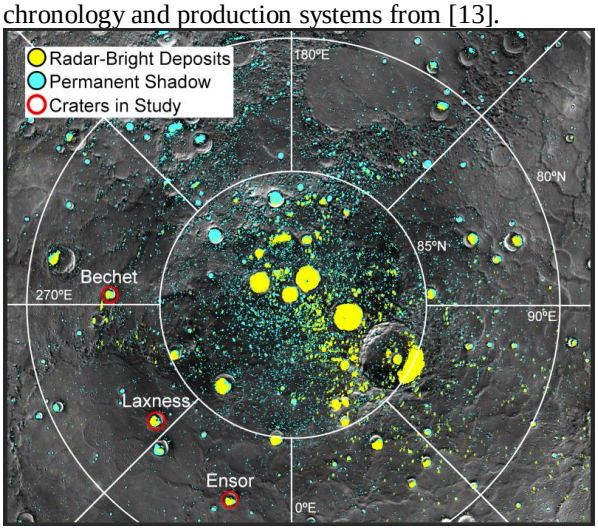

Fig. 1. *Distribution of water ice at the north polar region of Mercury, from 80°–90°N [14]. Regions of permanent shadow [14] are shown in blue and radar-bright materials [1] are shown in yellow. Craters analyzed in this study are outlined in red. Map is a MDIS mosaic in polar stereographic projection [14].*

Spatial heterogeneity measurements for ice deposits on the Moon. We explore the relationship between the spatial heterogeneity of ice and the age of host craters at the lunar poles in order to discuss the timing of volatile delivery to the Moon (Fig. 2). The spatial heterogeneity of a polar deposit is quantified as the percent of the cold trap occupied by ice. We define cold traps as regions with maximum surface temperatures ≤ 110 K, as measured by the Diviner Lunar Radiometer Experiment [15]. To determine what percent of cold traps are occupied, we use maps of surface water-ice detections derived from 1.4, 1.9, and 2.0 μm water absorptions measured by the Moon Mineralogy Mapper (M3) [16]. The ages of host craters are estimated by crater counting techniques [17].

Results: *Age estimates of water-ice deposits on Mercury.* The estimated derived ages for the ice surfaces within Laxness, Bechet, and Ensor craters are 38 ± 10 Myr, 65 ± 30 Myr, and 210 ± 60 Myr, respectively. These ages are slightly higher than, but within the error range of, the 50 Myr age that is predicted for the ice deposits by regolith gardening models [18]. The ages estimated here are also consistent

with the sharp albedo boundaries of ice deposits on Mercury, which suggest that the ice was deposited relatively recently or that a regularly refreshing mechanism exists [3, 10]. Additionally, these ages are consistent with the ice being delivered by a single, young impactor, such as the Hokusai impactor [19].

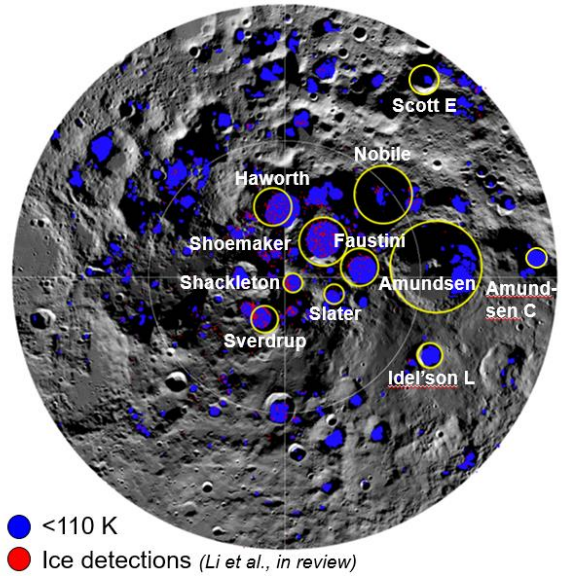

Fig. 2. *Distribution of surface water ice is shown in red for the south polar region of the Moon, from 80°–90°S [16]. Present-day cold traps are mapped in blue from Diviner maximum surface temperatures [14]. Craters analyzed in this study are outlined in yellow. Map is a LRO mosaic in polar stereographic projection.*

Spatial heterogeneity measurements for ice deposits on the Moon. We find that the degree of patchiness of lunar surface ice within a given PSR may be affected by the age of the cold traps. Specifically, we find three major populations of ice distribution: (1) Population 1 consists of ancient craters (>3.8 Ga) that tend to host the most patchy surface ice deposits, (2) Population 2 consists of middle-aged craters (between 2.9 and 3.8 Ga) that tend to host the most spatially coherent surface ice deposits, and (3) Population 3 consists of the youngest craters (<2.5 Ga), which do not show evidence for surface water-ice deposits [16].

Our results suggest that older ice deposits may have undergone higher rates of impact bombardment [8–9], contributing to a more patchy distribution of surface ice. Population 1 is consistent with relatively high impact rates [20], which is suggestive of not only high ice delivery rates, but also high impact destruction rates, where ice deposits are expected to be broken up and buried with time. Population 2 is consistent with a drop-off in impact delivery [20], where ice is still being delivered to the poles, but the ice also experiences relatively less impact destruction. Finally, Population 3 suggests that surface ice was not delivered at high rates after 2.5 Ga.

We also find that there are some ancient craters that are present-day cold traps, but do not host surface ice deposits. It is possible that this is an artefact of lunar true polar wander (TPW), or a physical reorientation of the spin axis relative to the Moon's present-day poles [e.g., 21]. Maps of the lunar poles when the Moon was on its paleo-axis [21] suggest that the specific craters that lack surface ice [16] may not have been stable cold traps for surface ice during the Moon's early history. Thus, our results suggest that surface ice patchiness observed at the lunar poles today may be controlled by ice supply rate, impact destruction rate, and TPW.

Implications: The same impact bombardment and space weathering processes operate on Mercury and the Moon, and Mercury's regolith may be overturned even more frequently than the lunar regolith [22]. The lack of apparent degradation of Mercury's ice deposits further suggests that the ice deposits on Mercury may be relatively young. As with the Moon, impact delivery rates on Mercury were higher during the planet's early history. Thus, it is possible that relatively ancient, degraded ice deposits exist in Pre-Tolstojan, Tolstojan, and Calorian craters (4.0–1.9 Gyr) below the coherent, pure deposits observed on Mercury's surface today.

In conclusion, we suggest that the spatial heterogeneity and purity of the Moon's polar deposits within a given PSR may be explained by relatively ancient deposition of ice, in comparison to relatively recent delivery of ice to Mercury's polar cold traps.

References: [1] Harmon J.K. et al. (2011) *Icarus, 211,* 37–50. [2] Butler B.J. et al. (1993) *JGR, 98,* 15003–15023. [3] Chabot N.L. et al. (2014) *Geology, 42,* 1051–1054. [4] Neumann G.A. et al. (2013) *Science, 339,* 296–300. [5] Colaprete A. et al. (2010) *Science, 330,* 463–468. [6] Schultz P.H. et al. (2010) *Science, 330,* 468–472. [7] Hayne P.O. et al. (2015) *Icarus, 225,* 58–69. [8] Pieters C.M. and Noble S.K. (2016) *JGRP, 121,* 2016JE005128. [9] Hurley D.M. et al. (2012) G*RL, 39,* L09203. [10] Chabot N.L. et al. (2016) *GRL, 43,* 9461–9468. [11] Deutsch A.N. et al. (2018) *Icarus, 305,* 139–148. [12] Michael G.G. and Neukum G. (2010) *EPSL, 294,* 223–229. [13] Neukum G. et al. (2001), *PSS, 49,* 1507–1521. [14] Deutsch A.N. et al. (2016), *Icarus, 280,* 158–171. [15] Paige D.A. et al. (2010) *SSR, 150,* 125–160. [16] Li et al. (2017) *ESF,* Abstract #NESF2017-135. [17] Tye A.R. et al. (2015) *Icarus, 255,* 70–77. [18] Crider D. and Killen R.M. (2005), *GRL, 32,* L12201. [19] Ernst C.M. et al. (2016) *LPS, XLVII,* Abstract #1374. [20] Nesvorný, D. et al. (2017) *Astron. J., 153,* 103. [21] Siegler, M.A. et al. (2016), *Nature, 531,* 480–484. [22] Domingue D.L. et al. (2014) *SSR, 181,* 121–214.